

Cyclic surface deformation behaviour of ZrH₂-purified iron: effects of solute carbon, strain amplitude, strain rate and environment

WON-JONG LEE

Department of Materials Science and Engineering, Korea Advanced Institute of Science and Technology, Taejon 305-701, Korea

M. E. FINE, Y. W. CHUNG

Department of Materials Science and Engineering, Northwestern University, Evanston, IL 60201, USA

The surface deformation behaviour in ZrH₂-purified interstitial-free iron was studied during fatigue in the push–pull plastic strain control mode under various combinations of plastic strain amplitude (5×10^{-4} , 5×10^{-3}), strain rate (5×10^{-4} , $3 \times 10^{-2} \text{ s}^{-1}$) and environment (ultrahigh vacuum, oxygen). Comparative tests of vacuum-melted commercially pure iron (CPI) containing 170 p.p.m. C were also conducted to investigate the effect of interstitials. At a plastic strain amplitude of 5×10^{-4} , the environmental effect is clearly exhibited regardless of the strain rate and the presence of interstitials. Fatigue in ultrahigh vacuum produces very fine slip lines not only in interstitial-free iron but also in vacuum-melted CPI. In the presence of oxygen, fatigue produces prominent slip lines, but those developed in CPI are more intense and coarser than those developed in interstitial-free iron. At the higher plastic strain amplitude of 5×10^{-3} , the gaseous environmental effect on the cyclic surface deformation is insignificant. The surface deformation behaviour is discussed in terms of the environmental effect and the basic mechanisms that govern the cyclic plasticity of iron.

1. Introduction

Although the fatigue properties of pure iron have been widely studied [1–9], little attention has been paid to the relationship between environmental effects and test conditions such as deformation amplitude and strain rate (or frequency). The effect of strain rate in cyclic deformation and fatigue behaviour of metals and alloys was reviewed by Laird and Charsley [10]. In fcc metals, the strain rate has little effect on the formation and propagation of fatigue cracks, and the cyclic flow stress is weakly dependent on it. In bcc metals, the strain rate is very important both in crystal deformation and in determining the failure mechanisms. At low strain rates, bcc metals are rather similar to fcc metals in their cyclic deformation. At high strain rates, however, the glide of edge dislocations predominates over that of screw dislocations which produces entirely different behaviour. The effect of strain rate on the initiation and propagation of fatigue cracks is also related to the interaction of the material with the environment because chemical effects are generally time-dependent. Coffin [11, 12] and Marchionni *et al.* [13] reported that, for a number of materials, the strong frequency effect found in air at high temperatures disappeared when the experiments were conducted in vacuum. Therefore, the intrinsic strain rate (or frequency) effect due to the rate sensitivity of the material should be differentiated from effects

caused by the interaction of the material with the environment.

In previous research [14] with vacuum-melted iron, fatigue deformation revealed a significant difference between ultrahigh vacuum (UHV) and oxygen environment in the cyclic surface deformation and the crack initiation mode. The difference was attributed to the transport of oxygen from the ambient to the metal through repeated slip motion during fatigue and subsequent weakening of the crystal. As is well known, impurity atoms play an important role in the plastic deformation of materials. The cyclic deformation behaviour of pure iron is markedly affected by the existence of small amounts of interstitials [8, 9]. Because not only the gaseous elements introduced by the repeated slip motion but also the interstitials in the bulk have influence on the motion of near-surface dislocations during fatigue, it is desirable to differentiate one effect from the other.

In the present research, the surface deformation behaviour in ZrH₂-purified interstitial-free iron is studied during fatigue in the push–pull plastic strain control mode under conditions of various combinations of plastic strain amplitude (5×10^{-4} , 5×10^{-3}), strain rate (5×10^{-4} , $3 \times 10^{-2} \text{ s}^{-1}$) and environment (UHV, oxygen). The results are compared with those obtained in vacuum-melted commercially pure iron (CPI) containing 170 p.p.m. C under the same test

conditions to reveal the effect of interstitials. The surface deformation behaviour is discussed in terms of the environmental effect and the basic mechanisms that govern the cyclic plasticity of iron.

2. Experimental procedure

The analysed impurity contents (wt %) of the pure iron used for these experiments are: 0.0013C, 0.023N, 0.003O, 0.0008S, and other elements such as magnesium, calcium, nickel, copper, aluminium, manganese and silicon are less than the detectable limits. Sheet-type fatigue specimens were prepared from the pure iron with gauge dimensions of 5 mm × 2.5 mm × 5 mm. They were subsequently chemically polished to remove the surface layer. In order to minimize the residual interstitials, the specimens were further purified for 200 h at 810 °C in a hydrogen atmosphere which was continuously purified by ZrH₂. The concentrations of carbon and nitrogen were expected to be less than 1 at p.p.m. [15]. The complete elimination of the yield point is another indication of the high interstitial purity of this ZrH₂-purified iron. The grain size after this treatment was 0.13 μm. After purification, they were polished with 1 μm diamond compound and then chemically polished in a solution of 95 vol % H₂O₂ (30% in water) and 5 vol % HF (48% in water) for a few seconds at room temperature. The ZrH₂-purified specimens were stored in a vacuum desiccator until testing.

A closed-loop computer-interfaced electrohydraulic fatigue apparatus was constructed and installed in an ultrahigh vacuum scanning Auger microprobe (SAM) equipped with ion sputtering and gas-handling facilities. A detailed description of the apparatus and electronics was presented elsewhere [16]. Fully reversed push-pull cycling ($R' = \epsilon_{\min}/\epsilon_{\max} = -1$) of ZrH₂-purified specimens were performed with constant plastic strain amplitudes $\Delta\epsilon_p/2$ of 5×10^{-4} and 5×10^{-3} using a triangular strain waveform and a constant total strain rate, $\dot{\epsilon}$, of $5 \times 10^{-4} \text{ s}^{-1}$. Cyclic plastic strains were measured and controlled with an axial MTS subminiature extensometer with a quick attachment device mounted on the gauge section of the specimen. In order to study the strain-rate dependence of cyclic deformation of the high-purity iron, cyclic tests were carried out at 10 Hz (which corresponds to the strain rate of $3 \times 10^{-2} \text{ s}^{-1}$) with a sinusoidal waveform under load control. Cyclic stress amplitude was continuously adjusted to obtain a constant plastic strain amplitude of 5×10^{-4} . Comparative tests of vacuum-melted CPI containing 170 p.p.m. C were also conducted to investigate the effect of interstitials on the cyclic surface deformation. CPI specimens with similar grain size (0.1 μm) were obtained by annealing at 850 °C for 1 h in vacuum ($1.3 \times 10^{-4} \text{ Pa}$) and furnace cooling. They were cycled under plastic strain control with a plastic strain amplitude of 5×10^{-4} and a total strain rate of $5 \times 10^{-4} \text{ s}^{-1}$. The environments employed in the present research were UHV ($6.5 \times 10^{-8} \text{ Pa}$) and oxygen (1 Pa). During evacuation of the chamber, zero strain condition was maintained by applying a tensile load

(0.18 kN) to counteract the atmospheric pressure. After the desired vacuum was achieved, the applied tensile load was set equal to a reference level of zero. Surface deformation was observed *in situ* by operating the SAM in the secondary electron detection mode and, after testing, with a standard scanning electron microscope or transmission electron microscope.

3. Results

Fig. 1 shows the variation of the average stress amplitude of ZrH₂-purified iron (a-c) and CPI (d) as a function of strain cycles. The cyclic stresses in these polycrystalline specimens both in UHV and in oxygen exhibit identical responses with cycling even though deformation markings on the surface are strongly affected by the environment. For a plastic strain amplitude of 5×10^{-3} and a strain rate of $5 \times 10^{-4} \text{ s}^{-1}$, rapid work hardening of ZrH₂-purified iron occurs at the beginning of the test and saturation is not achieved up to the cumulative plastic strain of 20 (Curve a). For the smaller plastic strain amplitude of 5×10^{-4} and the same strain rate of $5 \times 10^{-4} \text{ s}^{-1}$, cyclic stress amplitude also increases with the number of cycles, but the degree of hardening is much less (Curve c). With a cumulative plastic strain of 40, the cyclic stress amplitude is almost saturated at 74 MPa. The presence of interstitials causes a significant increase of the saturation stress, as expected. Note that the saturation stress amplitude of CPI containing 170 p.p.m. C is 120 MPa under the same test conditions (Curve d). It was found that the cyclic saturation stress of CPI is almost independent of the grain size. Curve b shows the cyclic stress response of ZrH₂-purified iron at the higher strain rate of $3 \times 10^{-2} \text{ s}^{-1}$ (10 Hz) and a plastic strain amplitude of 5×10^{-4} . The 60-fold increase of the

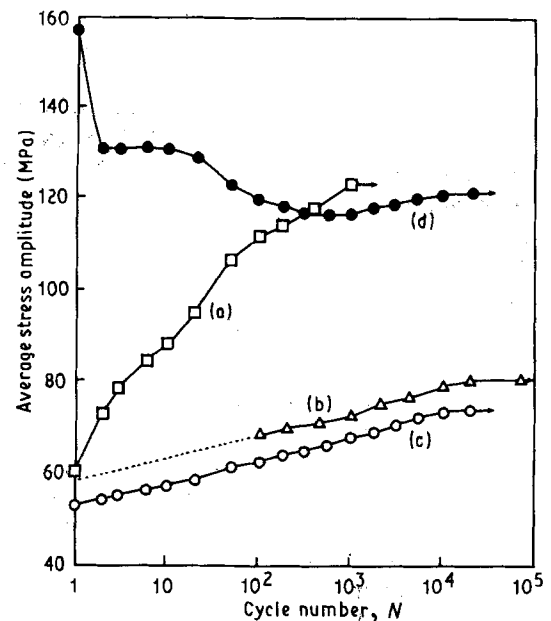


Figure 1 Cyclic stress response curves for (a-c) ZrH₂-purified iron and (d) vacuum-melted commercially pure iron. (a) $\Delta\epsilon_p/2 = 5 \times 10^{-3}$, strain rate = $5 \times 10^{-4} \text{ s}^{-1}$; (b) $\Delta\epsilon_p/2 = 5 \times 10^{-4}$, strain rate = $3 \times 10^{-2} \text{ s}^{-1}$ (10 Hz); (c, d) $\Delta\epsilon_p/2 = 5 \times 10^{-4}$, strain rate = $5 \times 10^{-4} \text{ s}^{-1}$. The cyclic stresses in these polycrystalline specimens exhibit identical responses with cycling both in UHV and in oxygen.

strain rate brings about an increase in the quasi-saturation stress level of about 10%. Error in adjusting the zero-level of load (≤ 0.03 kN) made it difficult to observe the stress differential effect between maximum stress in tension and maximum stress in compression.

Prior to fatigue testing, a 3 nm thick natural oxide layer (as estimated by the Auger depth profile technique) was removed from half of the gauge section surface by argon-ion sputtering. After thorough examination of the post-fatigue deformation of the surface with and without the natural oxide layer, we concluded that the natural oxide on iron does not play an important role in determining the cyclic surface deformation markings.

Fig. 2 shows scanning electron micrographs of the surfaces of purified iron specimens after 2×10^4 cycles at a plastic strain amplitude of 5×10^{-4} and a strain rate of $5 \times 10^{-4} \text{ s}^{-1}$. Fatigue testing in UHV causes very fine and wavy slip lines. These fine slip lines result from a rather uniform distribution of plastic deformation, resulting in the elimination of high strain concentration along slip lines. In oxygen, fatigue produced relatively well-developed slip lines as compared to those produced in UHV.

The post-deformation appearances of CPI specimens fatigued under the same test conditions in UHV and in oxygen are shown in Fig. 3. Slip lines produced in UHV are very fine, wavy and irregular, while those produced in oxygen are developed in a well-defined crystallographic direction along with the intense slip band cracks. The general surface deformation characteristics of CPI specimens are similar to those of the purified iron, but the effect of oxygen is more pronounced in CPI than in ZrH₂-purified iron; the slip lines developed in the iron containing solute carbon atoms are more coarse and distinct than those developed in the interstitial-free iron.

Fig. 4 shows scanning electron micrographs of the surfaces of purified iron specimens fatigued 2×10^4 cycles at a strain rate of $3 \times 10^{-2} \text{ s}^{-1}$ (10 Hz) in UHV and in oxygen. The plastic strain amplitude was controlled to $\pm 5 \times 10^{-4}$. At this higher strain rate, the specimen surfaces reveal much less severe cyclic deformation than they do at the lower strain rate of $5 \times 10^{-4} \text{ s}^{-1}$ (compare with Fig. 2), but grain-boundary damage is noticeable. The difference in the deformation features between UHV and oxygen atmospheres is again clearly exhibited. With further deformation at this higher strain rate, the originally shiny

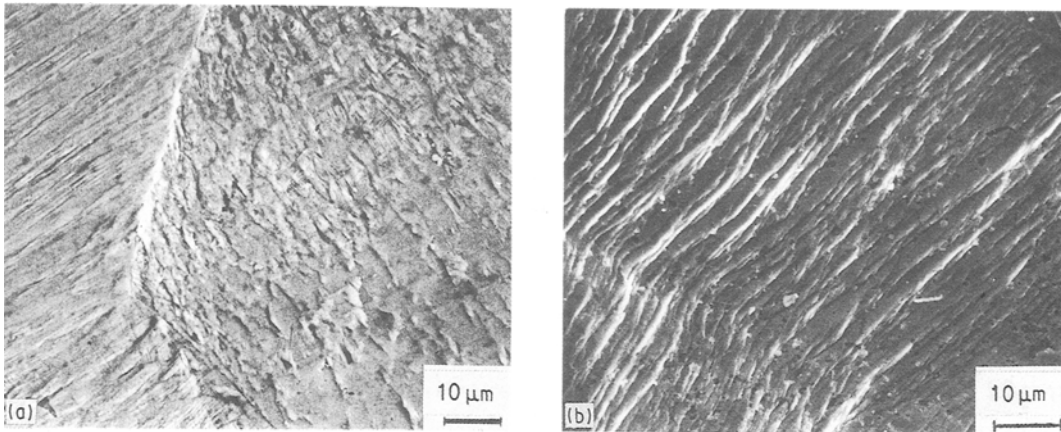


Figure 2 Scanning electron micrographs of surface deformation of ZrH₂-purified iron after 2×10^4 cycles at $\Delta\epsilon_p/2$ of 5×10^{-4} and strain rate of $5 \times 10^{-4} \text{ s}^{-1}$, (a) in UHV, (b) in oxygen (1 Pa).

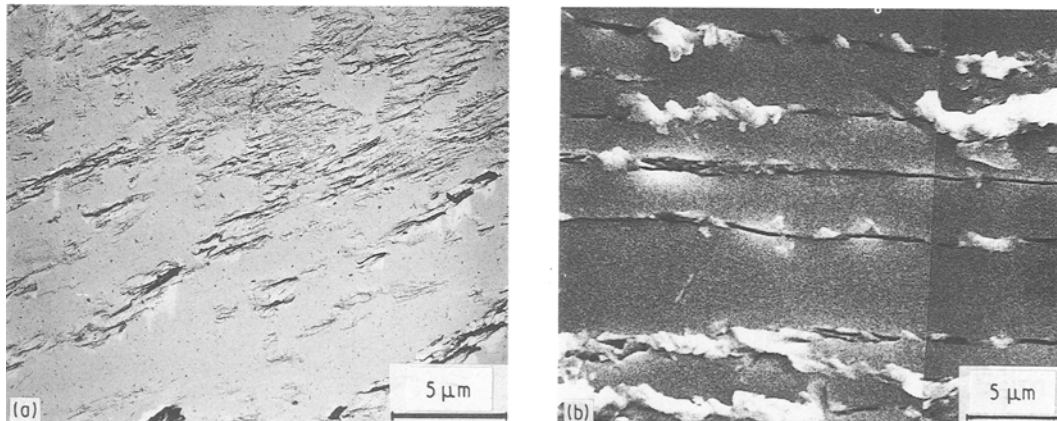


Figure 3 Surface deformation of vacuum-melted CPI after 2×10^4 cycles at $\Delta\epsilon_p/2$ of 5×10^{-4} and strain rate of $5 \times 10^{-4} \text{ s}^{-1}$, (a) in UHV (transmission electron micrograph of surface replica), (b) in oxygen of 1 Pa (scanning electron micrograph).

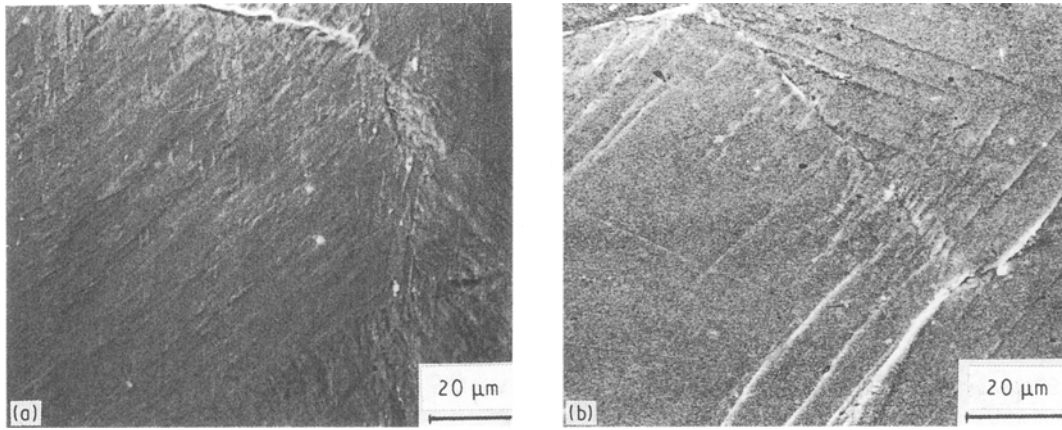


Figure 4 Scanning electron micrographs of surface deformation of ZrH_2 -purified iron after 2×10^4 cycles at $\Delta\epsilon_p/2$ of 5×10^{-4} and strain rate of $3 \times 10^{-2} s^{-1}$ (10 Hz), (a) in UHV, (b) in oxygen (1 Pa).

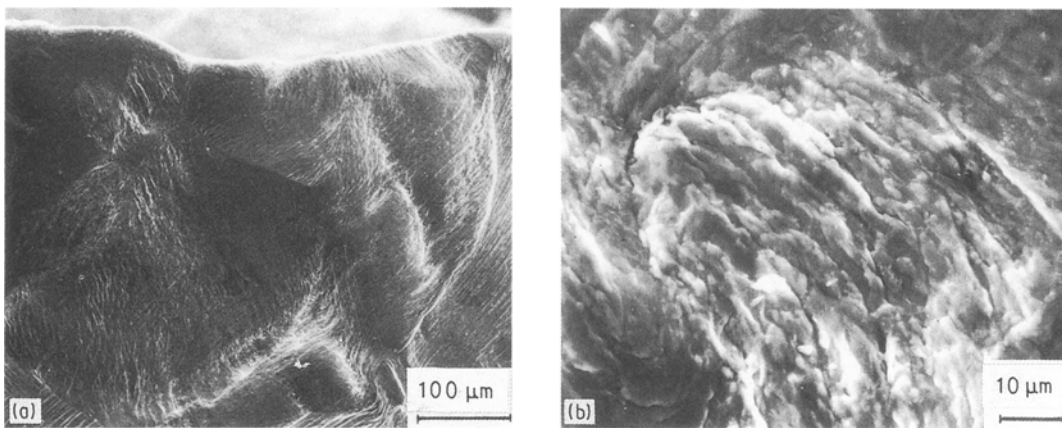


Figure 5 Scanning electron micrographs of surface deformation of ZrH_2 -purified iron after 8×10^4 cycles at $\Delta\epsilon_p/2$ of 5×10^{-4} and strain rate of $3 \times 10^{-2} s^{-1}$ (10 Hz) in UHV. (a) Low magnification, (b) high magnification.

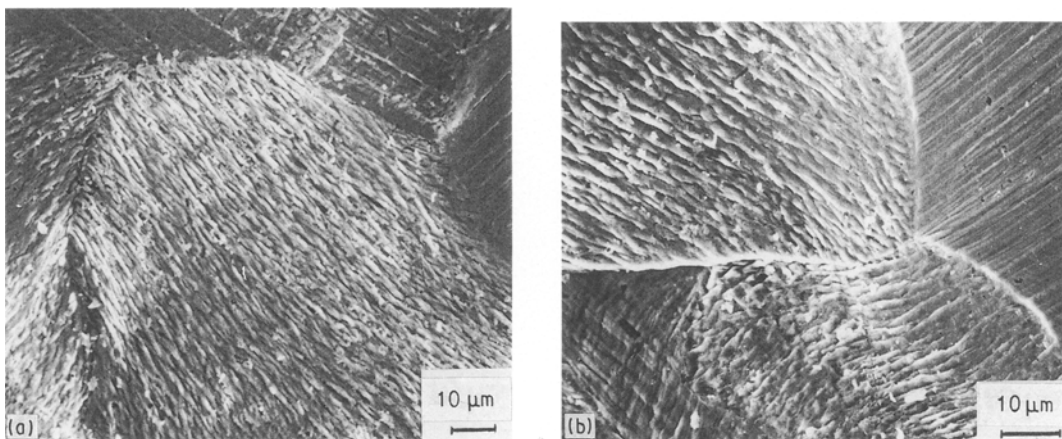


Figure 6 Scanning electron micrographs of surface deformation of ZrH_2 -purified iron after 400 cycles at $\Delta\epsilon_p/2$ of 5×10^{-3} and strain rate of $5 \times 10^{-4} s^{-1}$, (a) in UHV, (b) in oxygen (1 Pa).

surface becomes very dull and the wrinkling of the surface can be recognized with the naked eyes. The wrinkling of the surface results from shape changes of surface grains. Fig. 5 shows the surface deformation after 8×10^4 cycles in UHV.

It has been demonstrated that the effect of the environment on the formation of slip lines is appreci-

able at a plastic strain amplitude of 5×10^{-4} . In contrast, at the higher plastic strain amplitude of 5×10^{-3} , comparative observations reveal no significant difference between the cyclic surface deformation in UHV and that in oxygen atmosphere, as shown in Fig. 6. Fatigue testing in both media leads to the formation of well-developed slip lines.

4. Discussion

Cyclic deformation and fatigue behaviour in fcc and bcc metals have been extensively studied by Mughrabi *et al.* [6, 7, 17, 18]. In their treatment, the flow stress, σ , of a metal is expressed as the sum of an athermal component, σ_G , and an effective stress, σ^* , which depends on strain rate, $\dot{\epsilon}$, and temperature, T , [7]

$$\sigma = \sigma_G + \sigma^*(\dot{\epsilon}, T) \quad (1)$$

The athermal component, σ_G , is primarily due to the elastic interaction of dislocations during glide and is usually related to the dislocation density. In a bcc lattice, the lattice friction stress experienced by screw dislocations primarily contributes to the effective stress, σ^* , whereas, in an fcc lattice, σ^* is more dependent on dislocation interaction rather than lattice friction stress. For bcc metals, below a certain transition temperature T_0 , σ^* is considerably larger than σ_G and the Frank-Read type dislocation sources do not operate efficiently because of the impeded glide of screw dislocations. Above T_0 , σ^* becomes negligibly small as mobilities of screw and non-screw dislocations become more comparable, resulting in an overall behaviour similar to that of fcc metals. In the case of α -iron, T_0 lies above room temperature at strain rates of 10^{-4} s^{-1} or more. Hence in most cases (including the present experiments) the cyclic deformation of iron at room temperature would be controlled by the low-temperature deformation mode. However, Mughrabi *et al.* [6, 7] found that the addition of small amounts of solute interstitial atoms such as carbon could move the deformation mode into the high-temperature region and promote a behaviour similar to that of fcc metal. They observed "diffuse" slip lines from decarburized pure iron in air at room temperature, whereas iron containing 30 wt p.p.m. C showed coarse slip lines which are comparable to PSBs in fcc metals. It was proposed that carbon atoms interact with the non-screw dislocations to impede their mobilities and thus make the mobilities of screw dislocations comparable to those of non-screw dislocations, as in the high-temperature mode. However, in the present work, CPI containing 170 p.p.m. C as well as interstitial-free iron does not show any coarse slip lines in UHV. This finding is clearly in direct contradiction to the Mughrabi *et al.*'s contention that the bulk carbon atoms alone could change the fatigue deformation mode from the low-temperature mode to the high-temperature mode. It is strongly emphasized that one should be very cautious in applying results of surface observation to the interpretation of bulk behaviour, because the special characteristics of the surface and the interaction with the gaseous environment sometimes dramatically modify the appearance of surface features.

Majumdar and Chung [19] studied the effect of carbon content on the cyclic surface deformation behaviour of vacuum-melted commercially pure iron in UHV and oxygen. They suggested that fatigue-induced diffusion of oxygen into the metal may lead to the formation of oxygen-carbon clusters in the near surface region and the clusters, rather than oxygen or

carbon alone, control the surface deformation behaviour during fatigue. From the findings in the present research that (i) bulk carbon alone cannot produce coarse slip lines, and (ii) CPI containing 170 p.p.m. C shows more intense and coarser slip lines than interstitial-free iron, it is believed that carbon-oxygen clusters affect the dislocation motion and enhance the formation of coarse slip lines. However, it has been shown in the present research that the cyclic straining of the interstitial-free iron reveals a distinct difference in the surface deformation markings between in UHV and in oxygen, indicating that oxygen alone is also able to produce well-developed slip lines on the surface without carbon atoms. Therefore, it is concluded that oxygen alone (when solute carbon atoms are not present) or oxygen-carbon clusters (when carbon atoms are present) affect the dislocation motion and bring about the formation of coarse slip lines.

Gaseous environment has a substantial effect on the characteristics of the cyclic surface deformation. The environmental effects are clearly exhibited not only at the low strain rate of $5 \times 10^{-4} \text{ s}^{-1}$ but also at the high strain rate of $3 \times 10^{-2} \text{ s}^{-1}$ (10 Hz). The slip planes which intersect the specimen surface are the selective sites for chemical attack in iron when fatigued in oxygen. From the view that there would be less time for environmental attack at the higher frequency, one may expect that the environmental effect would be reduced as the strain rate increases. However, the oxygen pressure of 1 Pa used in the present research is high enough to cover the freshly exposed surfaces of slip steps completely with oxygen every cycle even at the high strain rate. In the study of Majumdar and Chung [20, 21], an oxygen pressure as low as $2.7 \times 10^{-4} \text{ Pa}$ was found to be sufficient to cause a distinct environmental effect at a cyclic frequency of 15 Hz in a reverse bending fatigue test. Therefore, the current observation of the environmental effect at the higher strain rate is not at all surprising.

Most materials exhibit hysteresis or dissipation of free energy on cycling even within the range normally thought of as elastic unless the frequency is very low (isothermal straining) or very high (adiabatic straining) [22]. At a strain rate of $5 \times 10^{-4} \text{ s}^{-1}$, the area enclosed by the hysteresis loop is extremely small when a specimen is cycled in elastic range, indicating that the cycle is almost isothermal. With increasing strain rate, the area of the hysteresis loop increases and the strain range at zero stress is no longer zero even within the elastic range. Because of this time-dependent elastic damping, the net irreversible plastic strain is smaller at the higher strain rate even though the strain range at zero stress is maintained the same, resulting in the less severe surface deformation at the higher strain rate.

At a plastic strain amplitude of 5×10^{-4} , the environmental effect is clearly exhibited regardless of the strain rate and the presence of interstitials. However, at the higher plastic strain amplitude of 5×10^{-3} , its effect on the cyclic surface deformation is insignificant. Alekseev and Grinberg [23] proposed that vacuum promotes the reduction of the activation stress of dislocation sources. According to their proposal, at

low strain amplitudes, many near-surface dislocation sources operate in UHV causing the high density of fine slip lines, whereas in oxygen, only a small number of active near-surface dislocation sources gives rise to the low density of slip lines. At high strain amplitudes, the applied stress is high enough to activate a large number of dislocation sources regardless of the environmental conditions, resulting in the high density of slip lines both in UHV and in oxygen. The present observation is in good agreement with the previous finding in HSLA steels [24] that the effect of gaseous environment is strongly dependent on the plastic strain amplitude and becomes insignificant as the plastic strain amplitude increases.

5. Conclusions

The surface deformation behaviour of ZrH₂-purified interstitial-free iron was studied during fatigue in the plastic strain-controlled mode under various combinations of plastic strain amplitude (5×10^{-4} , 5×10^{-3}), strain rate (5×10^{-4} , $3 \times 10^{-2} \text{ s}^{-1}$) and environment (UHV, oxygen). Comparative tests of vacuum-melted CPI containing 170 p.p.m. C were also conducted to investigate the effect of interstitials.

At the low plastic strain amplitude of 5×10^{-4} , fatigue in UHV produces very fine slip lines not only in interstitial-free iron but also in vacuum-melted CPI. This indicates that bulk carbon alone does not change the fatigue deformation mode. In the presence of oxygen, fatigue produces prominent slip lines, but those developed in CPI are more intense and coarser than those developed in interstitial-free iron. From these findings, it is concluded that oxygen alone (when solute carbon atoms are not present) or oxygen-carbon clusters (when carbon atoms are present) affect the dislocation motion and bring about the formation of coarse slip lines.

At the high strain rate of $3 \times 10^{-2} \text{ s}^{-1}$, the environmental effects are still clearly exhibited. At the high plastic strain amplitude of 5×10^{-3} , the gaseous environmental effect on the cyclic surface deformation is insignificant.

Acknowledgements

The authors thank Dr S. P. Bhat and R. Cline, Inland Steel Research Laboratory, for many helpful discussions.

References

1. R. P. WEI and A. J. BAKER, *Phil. Mag.* **12** (1965) 1005.
2. J. T. McGRATH and W. T. BRATINA, *ibid.* **12** (1965) 1293.

3. F. V. LAWRENCE Jr and R. C. JONES, *Met. Trans.* **1** (1970) 367.
4. M. SUGANO and K. KOJIMA, *J. Soc. Mater. Sci. Jpn* **19** (1970) 656.
5. *Idem., ibid.* **21** (1972) 846.
6. H. MUGHRABI, F. ACKERMANN and K. HERZ, ASTM-STP **675** (American Society for Testing and Materials, Philadelphia, PA, 1979) 69.
7. H. MUGHRABI, K. HERZ and X. STARK, *Int. J. Fract.* **17** (1981) 193.
8. S. HORIBE, R. SAGAWA, T. FUJITA and T. ARAKI, *Trans. Iron Steel Inst. Jpn* **20** (1979) 599.
9. K. MARUYAMA, M. MESHII, and H. OIKAWA, in "Proceedings of the 7th International Conference on the Strength of Metals and Alloys", Montreal, Canada Vol. 1 (1985) p. 373.
10. C. LAIRD and P. CHARLESLEY, in "Proceedings of the Conference on Ultrasonic Fatigue", Champion, October 1981, edited by J. M. Wells, O. Buck, L. D. Roth and J. K. Tien (Metallurgical Society of AIME, 1982) p. 187.
11. L. F. COFFIN Jr, *Met. Trans.* **3** (1972) 1777.
12. *Idem.*, in "Proceedings of the International Conference on Fatigue: Chemistry, Mechanics and Microstructure" (NACE, 1972) p. 590.
13. M. MARCHIONNI, D. RANUCCI and E. PICCO, in "Proceedings of the Conference on High Temperature Alloys for Gas Turbines", Liege, Belgium (1982) p. 791.
14. J. W. LEE, Y. W. CHUNG and M. E. FINE, *Met. Trans.* **19A** (1988) 337.
15. D. F. STEIN, J. R. LOW Jr and A. U. SEYBOLT, *Acta Metall.* **11** (1963) 1253.
16. W. J. LEE, Y. W. CHUNG and M. E. FINE, *Rev. Sci. Instrum.* **57** (1986) 2854.
17. H. MUGHRABI, K. HERZ and X. STARK, *Acta Metall.* **24** (1976) 659.
18. H. MUGHRABI, K. HERZ and F. ACKERMANN, in "Proceedings of the 4th International Conference on Strength of Metals and Alloys", Nancy (1976) Vol. 3, p. 1244.
19. D. MAJUMDAR and Y. W. CHUNG, *Mater. Sci. Engng* **67** (1984) 207.
20. *Idem., Scripta Metall.* **16** (1982) 791.
21. *Idem.*, in "Proceedings of the 2nd International Symposium on Defects, Fracture and Fatigue" (1982) edited by G. C. Sih and J. W. Provan (Martinus Nijhoff, The Hague, The Netherlands, 1983) p. 373.
22. I. HONG, in "Proceedings of the 4th National Congress on Pressure Vessel and Piping Technology: Random Fatigue Life Prediction", Portland, June 1983, edited by Y. S. Shin and M. K. Au-Yang (American Society of Mechanical Engineers, New York, 1983) p. 121.
23. A. I. ALEKSEEV and N. M. GRINBERG, *Fiz.-Khim. Obrab. Mater.* (1976) 98.
24. W. J. LEE, S. P. BHAT, Y. W. CHUNG and M. E. FINE, in "Proceedings of the 3rd International Conference on Fatigue and Fatigue Thresholds: Fatigue '87", Vol. III Charlottesville, June 1987, edited by R. O. Ritchie and E. A. Starke, Jr (EMAS, UK, 1987) p. 1211.

Received 10 July 1990

and accepted 6 February 1991